3D MODELLING OF THE WWER 440 HORIZONTAL STEAM GENERATOR

by

Vladimir D. STEVANOVIĆ and Milovan Ž. STUDOVIĆ

Original scientific paper
UDC: 621.039.5:621.18:519.876.5
BIBLID: 0354–9836, *2* (1998), 1, 103–122

A three-dimensional thermal-hydraulic model and a numerical procedure for the simulation and analysis of steady-state as well as transient operation of horizontal steam generators are presented. The two-fluid modelling approach is applied for the two-phase flow on the shell side of the steam generator. The model is solved by the SIMPLE numerical procedure, which has been adjusted for the multiphase flow conditions. The operation of the horizontal steam generator in the WWER 440 nuclear power plant has been simulated at the full load, steady-state condition. Presented results are compared with the data measured at the NPP Novovoronezh. The agreement is good. Obtained results can be used in plant design or retrofitting, in nuclear power plant safety analyses and as improvement of existing one- dimensional thermal-hydraulics models of the horizontal steam generator which are assessed by system codes used for the nuclear power plant safety analyses.

Introduction

Thermal-hydraulic processes in the horizontal steam generators (HSGs) built in the Russian type nuclear power plants with light water reactors WWER 440 and 1000 have been the subject of considerable safety analyses during the last decade. Experimental data on the HSG behaviour are limited, especially the data about the complex three-dimensional two-phase flow conditions on the HSG shell side. The assessment of HSG operational conditions with the system codes used for the nuclear power plant safety analyses, such as RELAP5, CATHARE, RETRAN and others [1], still have to be validated, because of the one- dimensional nature of thermal-hydraulic flow models built into these codes. Therefore, there is a need for detailed three-dimensional simulations and analyses of HSG thermal-hydraulics during nominal, partial loads, and transient operation, as well as under accident conditions.

The horizontal steam generator in the nuclear power plant WWER 440 has a unique design. The HSG vessel is cylindrical. Reactor coolant is flowing through horizontal U-tubes, which extend from a hot (inlet) header towards a cold (outlet) header. The headers are positioned in a short distance vertically and asymmetrically near the half

length of the HSG, (Figs. 1 and 3). Tubes are closely packed in two central and two peripheral tube bundles, with narrow free passages between the bundles, (Fig. 2). The feedwater is injected through a sprayer into the middle of the tube bundle (Fig. 3), where it mixes with a low quality two-phase mixture and by mechanism of steam condensation it is heated up to the temperature of steam saturation. Liquid and steam separation occurs primarily by gravity. Two-phase mixture swell level is located slightly above the top of the tube bundles. The HSG design leads to the freely self-organised loops of two-phase mixture

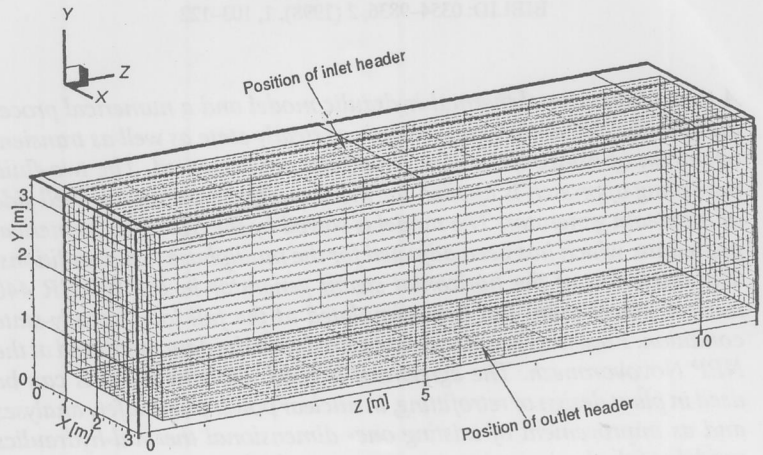

Figure 1. Grid used for the numerical simulation of WWER 440 HSG

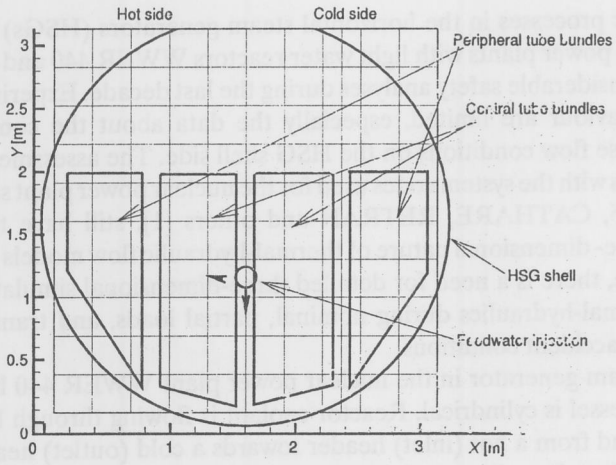

Figure 2. Grid in X-Y plane used for the numerical simulation of WWER 440 HSG

natural circulation on the shell side of the HSG. Main WWER 440 HSG operating parameters are as follows. The nominal thermal capacity is 230 MJ/s with corresponding steam production of 126 kg/s. The shell side pressure is 4.6 MPa. The feedwater temperature is 223 °C, while the primary coolant parameters are reactor coolant flow rate of 1390 kg/s and reactor coolant inlet and outlet temperature 300/269 °C. The total heat transfer surface is 2577 m^2, formed by 5536 tubes with tube dimension 16 × 1.4 mm.

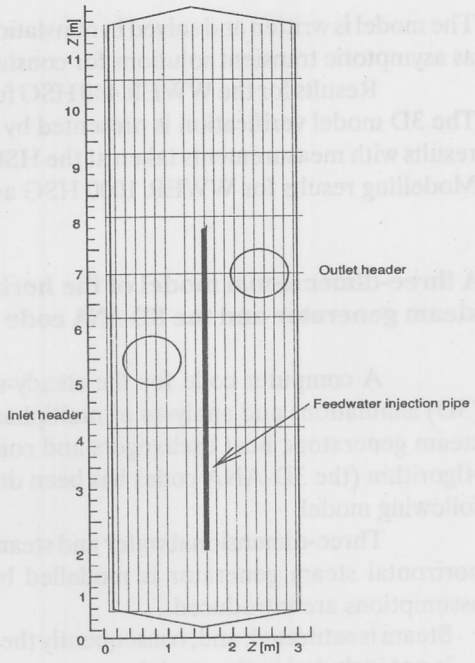

Figure 3. Grid in *X–Z* plane used for the numerical simulation of WWER 440 HSG

So far as the authors are aware, there are only two published papers on the three-dimensional modelling of HSG thermal-hydraulics, [2, 3]. Groburov and Zorin [2] reported on the three-dimensional modelling of the WWER 1000 HSG shell side two-phase flow within the tube bundles, without consideration of the steam dome and flow in the HSG edges. Two-phase flow interaction was incorporated through drift-flux velocity. It was assumed that there is no steam cross flow and two-phase flow acceleration was neglected in the two-phase mixture momentum equation. Melikhov *et al.* [3] developed a transient, compressible, two-fluid model, which was applied to both WWER 440 and 1000. Their numerical data show higher void fraction values than experimentally observed in case of WWER 1000 modelling.

Here, a three-dimensional (3D) model is presented, developed in order to simulate steady- state, as well as transient HSG thermal-hydraulic behaviour during full load, partial load and operational, as well as abnormal transient conditions. Obtained results can be used in plant design or retrofitting, in nuclear power plant safety analyses and as improvement of existing one-dimensional thermal hydraulic models of the HSG which are assessed by system codes in nuclear industry.

Three-dimensional water and steam two-phase flow on the secondary side of the horizontal steam generator is modelled by the "two-fluid" model. Mass and momentum conservation equations are written for each phase, while energy conservation equation is written only for water due to the assumption about steam saturated conditions. "Closure laws" are prescribed for mass, momentum and thermal energy transfer at steam-water interfaces, as well as for tube flow resistance, energy transfer and steam generation within tube bundles. The model is solved by the SIMPLE numerical procedure, which has been extended in order to take into account the 3D flow of two fluid phases – water and steam.

The model is written and solved in nonstationary form, while steady states are determined as asymptotic transient solutions for constant boundary conditions.

Results for the WWER 440 HSG full load, steady-state conditions are presented. The 3D model verification is presented by comparing numerical steam volume fraction results with measurements taken at the HSG of the Novovoronezh Nuclear Power Plant. Modelling results for WWER 1000 HSG are presented elsewhere [4, 5].

A three-dimensional model of the horizontal steam generator and the 3D-ANA code

A computer code for the steady-state, as well as transient three-dimensional (3D) simulations and analyses of multiphase flows in power plant components, such as steam generators, heat exchangers and condensers, based on the *A*dvanced *N*umerical *A*lgorithm (the 3D-ANA code) has been developed. The 3D-ANA code is based on the following model.

Three-dimensional water and steam two-phase flow on the secondary side of the horizontal steam generator is modelled by the "two fluid" model [6]. The following assumptions are introduced.

- Steam is saturated, and, consequently the steam thermal energy conservation equation is not included in the model.
- There is no heat transfer between the steam and steam generator tubes.
- Pressure is the same for both phases within the numerical control volume.
- Tube bundles flow resistance is assumed to be uniformly distributed and the porous medium concept is used in the simulations of two-phase flow through tube bundles.
- Flow governing equations are written in the nonviscous form, while the turbulent viscosity effects are taken into account indirectly through friction coefficients for the tube bundles flow resistance and two-phase interfacial shear.

Conservation equations for the two-phase water and steam flow on the HSG shell side

The 3D-ANA code is based on the mass and momentum conservation equations for water and steam and water thermal energy conservation equation. These equations have the following coordinate-free vector form.

Water mass conservation equation

$$\frac{\partial(\alpha_1\rho_1)}{\partial t} + \nabla(\alpha_1\rho_1\vec{u}_1) = -\Gamma_e + \Gamma_c + M_1 \tag{1}$$

Steam mass conservation equation

$$\frac{\partial(\alpha_2\rho_2)}{\partial t} + \nabla(\alpha_2\rho_2\vec{u}_2) = \Gamma_e - \Gamma_c \tag{2}$$

Water momentum conservation equation

$$\frac{\partial(\alpha_1\rho_1\vec{u}_1)}{\partial t}+\nabla(\alpha_1\vec{u}_1\vec{u}_1)=-\alpha_1\nabla p+\alpha_1\rho_1\vec{g}+\vec{F}_{21}-\vec{F}_{31}-(\Gamma_e-\Gamma_c)\vec{u}_{1i}+M_1\vec{u}_{FW} \quad (3)$$

Steam momentum conservation equation

$$\frac{\partial(\alpha_2\rho_2\vec{u}_2)}{\partial t}+\nabla(\alpha_2\rho_2\vec{u}_2\vec{u}_2)=-\alpha_2\nabla p+\alpha_2\rho_2\vec{g}-\vec{F}_{21}-\vec{F}_{32}+(\Gamma_e-\Gamma_c)\vec{u}_{1i} \quad (4)$$

Water energy conservation equation

$$\frac{\partial(\alpha_1\rho_1 h_1)}{\partial t}+\nabla(\alpha_1\rho_1 h_1\vec{u}_1)=\alpha_1\frac{\partial p}{\partial t}-(\Gamma_e-\Gamma_c)h''+M_1 h_{FW}+q_{31} \quad (5)$$

Projections of the momentum equations (3) and (4) onto the axes of the Cartesian coordinate system (x, y, z) give six scalar partial differential equations, (three eqs. per every phase). These equations together with mass and energy conservative equations (1) and (5) give a set of eight partial differential equations, with the following main dependant variables: water volume fraction (α_1), water velocity components (u_1, v_1, w_1), steam velocity components (u_2, v_2, w_2), water enthalpy (h_1). The sum of equations (1) and (2), together with the sum of momentum equations (3) and (4) are used for the derivation of the pressure correction equation in the same way as proposed by Patankar in the SIMPLE numerical method [7] for one-phase flow. The interface velocity $\vec{u}_{1i}$ in the momentum equations is assumed to be the water bulk velocity $\vec{u}_1$. Steam mass conservation eq. (2) is replaced by the simpler volume fraction balance, eq. (6), for the calculation of steam volume balance

Volume fraction balance

$$\alpha_1+\alpha_2+\alpha_3=1 \quad (6)$$

Energy balance equation for the reactor coolant flow on the primary side

Reactor coolant flow inside the U-tubes is modelled by the one-dimensional thermal energy conservation equation in the following form

$$\rho_1 c_{p,1}\left(\frac{\partial T_I}{\partial t}+u\frac{\partial T_I}{\partial x}\right)=-k(T_I-T_{II})\frac{S}{V} \quad (7)$$

where T_I is reactor coolant temperature, T_{II} is water temperature on the secondary, shell side around U-tubes and S/V is ratio of tube's inner wetted surface and volume per unit pipe length.

Closure laws

Mass, momentum and energy transfer at the steam and water interface, as well as between water and steam phases and tube bundles are determined with the closure laws, as follows.

Primary to secondary side heat transfer

Overall heat transfer coefficient (h.t.c.) k for the heat transfer from the hot water inside tubes of the tube bundle towards the two-phase mixture on the shell side of the HSG is calculated as

$$k = \left[\frac{1}{h_1} + R_w + \frac{1}{h_2}\right]^{-1} \tag{8}$$

where heat transfer coefficient inside tubes is calculated as

$$h_1 = 0.021 \frac{\lambda}{d} \mathrm{Re}^{0.8}\, \mathrm{Pr}^{0.43} \tag{9}$$

and heat transfer coefficient from tube to two-phase mixture is calculated by the correlations recommended for the steam generator shell side heat transfer [8]

$$h_2 = 4.32(p^{0.14} + 1.28 \cdot 10^{-2} p^2) q^{0.7} \tag{10}$$

where: h_2 [W/m^2 K], p [MPa], and q [W/m^2].

Steam water flow regimes

Steam volume fraction in the space occupied only by the two-phase mixture is determined according to the following expression

$$\varphi = \frac{\alpha_2}{\alpha_1 + \alpha_2} \tag{11}$$

The lack of the experimental evidence on the two-phase flow patterns inside the horizontal tube bundles and within the HSG complex geometry has led to a simple assumption about the two-phase flow patterns, as is presented in Table 1.

Table 1. The assumption about two-phase flow pattern

Bubbly flow	Transitional-Churn flow
$\varphi \leq 0.3$	$0.3 < \varphi \leq 1.0$

Interfacial momentum transfer

Calculation of the interfacial momentum transfer is a crucial step for a proper prediction of the relative velocities between the steam and water phase, and consequently the void fraction.

The interfacial drag force per volume of computational cell, which can comprise water, steam and tubes, is calculated as

$$\vec{F}_{ij} = \frac{3}{4}\alpha_i \rho_j \frac{C_D}{Dp}\left|\vec{u}_i - \vec{u}_j\right|(\vec{u}_i - \vec{u}_j) \tag{12}$$

where the indexes are as follows: $i = 2, j = 1$ for bubbly and churn flow pattern, and $i = 1, j = 2$ for droplet flow pattern.

Several correlations for interfacial drag coefficient have been considered in the investigation of 3D HSG modelling presented here. Ishii and Zuber [9] had proposed the following correlations for interfacial drag coefficient in dispersed and transitional two-phase flow regimes

- Churn flow ($0.3 < \varphi < 0.7$)

$$C_D = \frac{8}{3}(1-\varphi)^2 \tag{13}$$

$$D_p = 4\left\{\frac{g\Delta\rho}{\sigma}\right\}^{-1/2} \tag{14}$$

- Bubbly flow, $\varphi \leq 0.3$, and droplet flow, $\varphi \geq 0.7$

$$C_D = \frac{2}{3}D_p\left\{\frac{g\Delta\rho}{\sigma}\right\}^{1/2}\left\{\frac{1+17.67f(\varphi)^{6/7}}{18.67f(\varphi)}\right\}^2 \tag{15}$$

where
$f(\varphi) = (1-\varphi)^{1.5}$ for bubbly flow
$f(\varphi) = \varphi^3$ for droplet flow,
and dispersed particle diameter is calculated as

$$D_p = \frac{\sigma We_{cr}}{\rho_i\left|\vec{u}_1 - \vec{u}_2\right|^2} \tag{16}$$

where
i=1, We_{cr} = 8 for bubbly flow,
i=2, We_{cr} = 12 for droplet flow.

These correlations have been used by various investigators, for instance in steam explosion [10], as well as in horizontal steam generator calculations [3]. A number of calculations with the 3D-ANA code have been performed with the same correlations for the conditions of the HSG shell side two-phase flow. It has been shown that their use

leads to high interfacial drag force in the range of churn and droplet flow patterns, which results in too high values of steam volume fractions and liquid carry-over from the two-phase mixture pool towards the steam generator exit. The same conclusions about too high interfacial drag force calculated with the same correlations has been also reported recently by other authors [11].

The lower values of interfacial drag coefficient for churn and separated flow patterns were also reported by the CATHARE developing team in separated effects tests [12]. It was shown that the product of the interface surface and interfacial shear stress $(a_i\tau_i)$ is three to four orders of magnitude lower in transitional and annular flow than in the bubbly flow pattern. Especially, low value of $(a_i\tau_i)$ product is reported for counter-current steam water flow which is expected to take place in the HSG near the swell level where steam is leaving two-phase mixture and the water is changing the flow direction from the upward to the downward flow. In the reference [12] the product $(a_i\tau_i)$ for the transitional flow regime is represented with

$$(a_i\tau_i) = \xi\rho_1 \frac{(u_2 - u_1)^2}{D} \tag{17}$$

where $(u_2 - u_1)^2$ is the square of the steam and water vertical velocity difference in the tube, D is tube diameter and ξ is an interfacial friction factor determined experimentally with

$$\xi = 8.16\varphi(1-\varphi)^3(1-0.75\varphi)^2 \tag{18}$$

Equation (17) agrees with the common statement that interfacial momentum transfer is proportional to the square of the phases velocity difference. Equation (18) is purely empirical. It comprises both interfacial area and drag influence on the momentum transfer. Combining eqs. (12) and (17), and taking into account that $|\vec{F}_{ij}| = (a_i\tau_i)$ the following relation is obtained for the interfacial drag coefficient

$$C_D = \frac{4}{3}\frac{\xi D_p}{\varphi D} \tag{19}$$

From equations (18) and (19) it can be seen that the interfacial drag coefficient is proportional to the fifth power of $(1-\varphi)$, which means a higher reduction of the interfacial drag with a steam void increase than it is given with the Ishii and Zuber model, where interfacial drag is proportional to the second power of $(1-\varphi)$.

In the 3D-ANA code the interfacial drag force per unit volume between the water and steam, equation (12), is calculated with the Ishii and Zuber model for interfacial drag coefficient in bubbly flow pattern, eq. (15), and with the CATHARE model for transitional flow patterns – churn flow, which is extended up to the values of the steam void φ of 1, equations (18) and (19). Diameter D in correlation (19) is determined in order to obtain the agreement between calculated and available measured void fractions. Available experimental base for WWER 1000 HSG is wider than for

WWER 440 HSG. Therefore, the experimental data for WWER 1000 HSG, presented in reference [13], are taken for D values determination. Void fraction measurements at this steam generator are performed at 15 locations on the HSG shell side. In section 4 of this paper, it is shown that WWER 440 HSG available void fraction measurements were taken only at 5 locations on the HSG shell side. Numerical results of WWER 1000 HSG simulation with the 3D-ANA code are presented in [4] and [5]. Within the scope of these numerical simulations, a value of $D = 0.008$ m is determined for the flow inside tube bundles. The same values of D parameter are used for the WWER 440 HSG calculations. The value $D = 0.008$ m for the flow within the tube bundle corresponds to the minimum distance between two adjacent tube walls, *i. e.* to the minimum clearance between two tubes. Outer tube diameter is 0.016 m for both HSG. In WWER 1000 HSG tubes are arranged in triangular lattice, with 0.019 m pitch in vertical direction and 0.024 m tube pitch in horizontal direction. In this arrangement, the minimum distance between two tubes' walls is 0.0062 m. In WWER 440 HSG tubes in the bundle are arranged in a rectangular lattice with vertical pitch of 0.024 m and horizontal pitch of 0.030 m. In this arrangement the minimum distance between two tubes walls is in the vertical direction and has the value of exactly 0.008 m, *i. e.* the same value as it is determined for parameter D for flow within tube bundle. For flow outside tube bundles $D = 0.015$ m, which has no counterpart in the flow channels geometry.

Frictional pressure drop in tube bundles

Pressure drop due to two-phase mixture flow through the tube bundle is determined with the homogeneous model, taking into account the separate contribution of each phase to the total pressure drop. The pressure drop of the water flow in the direction of the e coordinate axis ($e = x, y, z$) is determined taking into account the volume occupied by the water $(1 - \varphi)$

$$\Delta p_{1,e} = \varsigma_e \frac{\rho_1 u_{1,e}^2}{2}(1-\varphi) \tag{20}$$

where ζ_e is pressure loss coefficient in the e direction. For the steam phase the similar equation is written

$$\Delta p_{2,e} = \varsigma_e \frac{\rho_2 u_{2,e}^2}{2}\varphi \tag{21}$$

Summing equations (20) and (21), the total pressure drop in homogeneous two-phase flow is obtained as presented in [14]

$$\Delta p_e = \varsigma_e \frac{G^2}{2\rho_1}\left[1 + x\left(\frac{\rho_1}{\rho_2} - 1\right)\right] \tag{22}$$

where total mass flux is given with

$$G = (1 - \varphi)\rho_1 u_1 + \varphi\rho_2 u_2 \tag{23}$$

Pressure loss coefficient ζ_e is calculated with the experimental correlations proposed in [8] for the HSG tube bundle with rectangular tubes' arrangement

$$\varsigma_e = (6 + 9z_t)\,\mathrm{Re}^{-0.26}\left(\frac{s}{d}\right)^{-0.23} \tag{24}$$

where z_t is the number of tube rows in the observed x, y or z direction within the computational cell, Re is Reynolds number determined with the pipe outer diameter (d) and the maximum phase velocity at the minimum flow area between tubes in the observed direction, and s is tube pitch.

Tube wall-fluid drag force is calculated as follows

$$\vec{F}_{3i} = \frac{\Delta p_{i,e}}{\Delta e}\vec{e} \tag{25}$$

where Δe is the width of the computational cell in the e direction ($e = x, y, z$), $\vec{e}$ denotes unit vector and index $i = 1, 2$.

Interfacial phase change

The evaporation and condensation at the water and steam interface are calculated with a simple empirical model which takes into account the phase change relaxation time. The evaporation rate is calculated when the water enthalpy is greater than water saturation enthalpy, *i. e.* $h_1 > h'$ with the following correlation [3]

$$\Gamma_e = \frac{\alpha_1\rho_1}{\tau}\frac{h_1 - h'}{h'' - h_1} \tag{26}$$

Otherwise, when $h_1 \le h'$, there is no evaporation. Condensation within numerical cell takes place according to the physical condition that steam is in contact with subcooled water, *i. e.* $h_1 < h'$ and $\alpha_2 > 0$. Condensation rate is calculated as

$$\Gamma_c = \frac{\alpha_1\rho_1}{\tau}\frac{h' - h_1}{h'' - h_1} \tag{27}$$

Melikhov *et al.* [3] have not given any evidence about the consideration of the condensation process in their model of horizontal steam generator, even for the space of direct subcooled feed water injection in the two-phase mixture on the shell side of the HSG. A similar empirical correlation, comprising relaxation time τ, as it is written in equation (26) is used in the THYC code, developed and applied by the EdF to heat exchangers and vertical steam generators thermal-hydraulic calculations [15].

Space discretization and numerical method

The SIMPLE numerical procedure [7] has been applied for the numerical solution of the set of eight scalar conservative equations, which results from scalar eqs. (1) and (5) and projections of two momentum vector eqs. (3) and (4) onto Cartesian coordinate axes. The discretization of these partial differential equations is carried out by integrating them over control volumes in a staggered grid. Water enthalpies and volume fractions are calculated in scalar control volumes, while velocities are calculated in staggered momentum control volumes. According to the SIMPLE procedure, the equations are linearized. The convective terms are approximated with upwind finite differences. A fully implicit time integration is applied. The resulting discretized equations are solved in primitive variables iteratively. For the calculation of a steady-state condition, the transient calculation procedure is performed with constant boundary conditions, in the following steps:

(1) Void volume fraction and water enthalpy are calculated for scalar control volumes from a set of equations resulting from eqs. (1) and (5).
(2) Water and steam velocity components are calculated for staggered momentum control volumes, from a set of equations resulting from projections of eqs. (3) and (4).
(3) Pressure equations, obtained by the SIMPLE procedure, are solved for scalar control volumes.
(4) Time is increased, new values are taken as initial ones for the new time step of integration and the physical properties are updated with new values of dependant variables.
(5) Steps 1 to 4 are repeated until the total water and steam mass conservation, sum of eqs. (1) and (2), is achieved within the prescribed error for every scalar control volume (less than 0.1 kg/s in several consecutive calculation loops).

The solution of the sets of linear algebraic equations within steps 1, 2, and 3 is performed with the Three-Diagonal-Matrix-Algorithm (TDMA) procedure [7], with three to five inner iterations, while one iteration comprises the forward and backward solution along all three Cartesian axes.

The satisfaction of the total water and steam mass balance for the every scalar control volume, step 5, implies also that the overall mass balance, for the whole HSG is achieved in the steady-state conditions. The relative difference between prescribed feedwater inlet mass flow rate and calculated steam outlet mass flow rate is less than 1%.

Modelling of WWER 440 HSG

A WWER 440 horizontal steam generator (HSG) operation at full, 100% load is simulated with the 3D-ANA code. A numerical grid with $21 \times 21 \times 11$ (= 4851) control volumes is used for the numerical simulation as shown in Fig. 1. The HSG geometry and numerical grid in X–Y plane is shown in Fig. 2, and in X–Z plane in Fig. 3. Cross sections of the grid lines in these figures are placed in the middle of the control volumes. The size,

position, and consequently the number of the control volumes have been chosen in order to model all main geometric characteristics of the HSG, to achieve required computational accuracy (as presented in the previous chapter), as well as to provide acceptable computational times for engineering calculations on a PC machine. A CPU time for the steady-state calculation with the above stated HSG discretization is less than 3 hours on the Pentium PC with 200 MHz processor.

Steam void fraction distribution is shown in Fig. 4 in several X–Y planes, where void fraction is determined as the steam volume fraction in the two-phase mixture $\varphi = \alpha_2/(\alpha_1 + \alpha_2)$. As it can be seen, in the lower part of the tube bundles void is between 0.1 and 0.3, in the middle and upper parts void is between 0.3 and 0.5, while only at the top tubes' rows void has slightly higher values than 0.5. The influence of the feedwater injection on the void distribution can be seen in Fig. 5, where isoline of low void 0.10 is risen toward the feedwater injection tube.

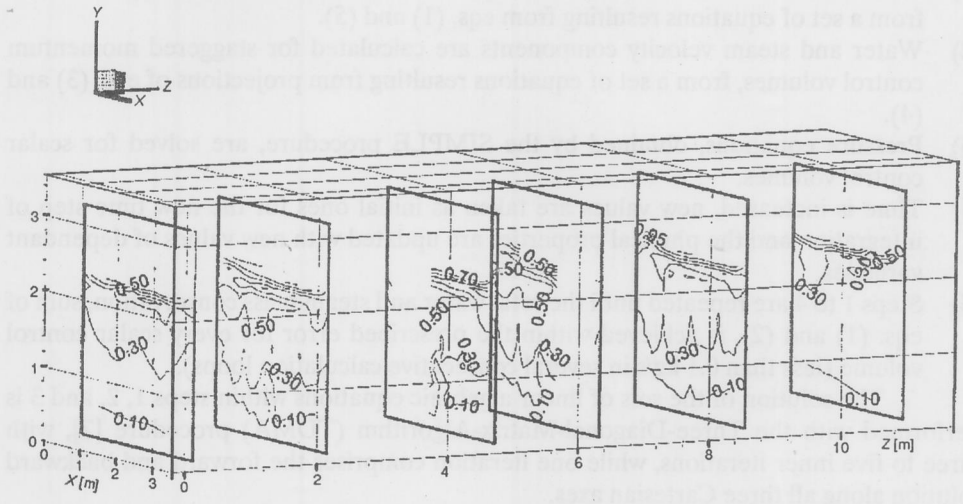

Figure 4. 3D view at void isolines in several X–Y planes for WWER 440 HSG

By using the results of water and steam velocity vectors and volume fractions, the phases mass flux vectors are calculated as $\vec{G}_i = \alpha_i \rho_i \vec{u}_i$, i = 1, 2, and presented in Figs. 6 to 9. These results indicate the spatial mass, momentum and energy transport by the water and steam on the shell side of the HSG. The water mass flux vectors in Figs. 7 and 8 show a water circulation in X–Y planes at positions z = 3.7 m and 8.8 m. A water downward flow from the swell level towards the tube bundles at z = 3.7 m concentrates on the passage between the peripheral bundle and the steam generator shell on the cold side, due to the much higher heat flux and steam generation on the hot side than on the

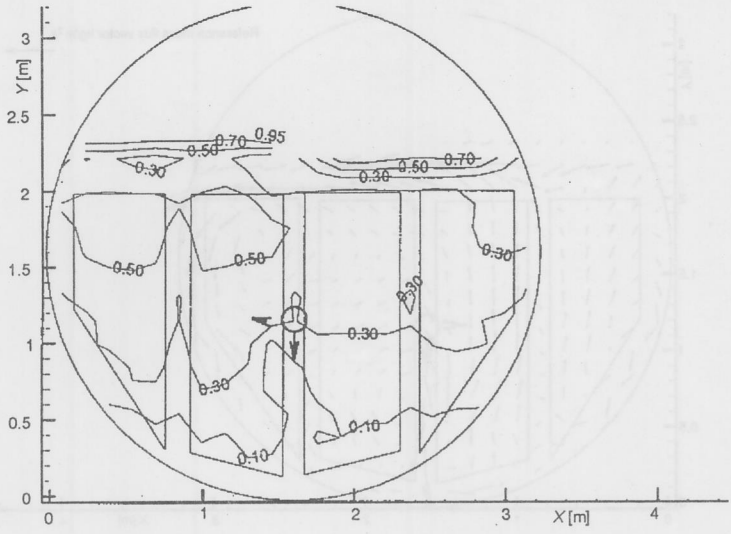

Figure 5. Void isolines in *X–Y* plane at $Z = 3.7$ m for WWER 440 HSG

cold side and higher upward two-phase flow velocities on the hot than on the cold side of the HSG, Fig. 6. This water downward flow leads to the steam void lower than 0.3 at the right upper part of the cold side peripheral tube bundle, as it is shown in Fig. 5. At

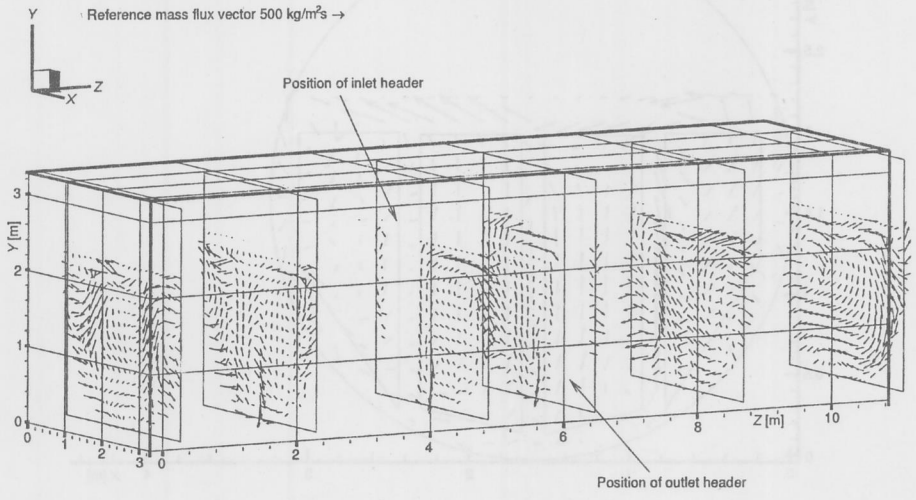

Figure 6. 3D view at water mass flux vectors in several *X–Y* planes for WWER 440 HSG

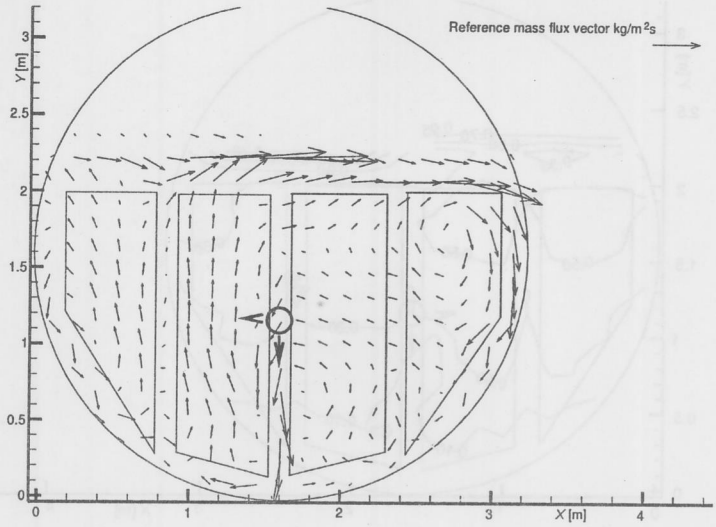

Figure 7. Water mass flux vectors in *X–Y* plane at $Z = 3.7$ m WWER 440 HSG

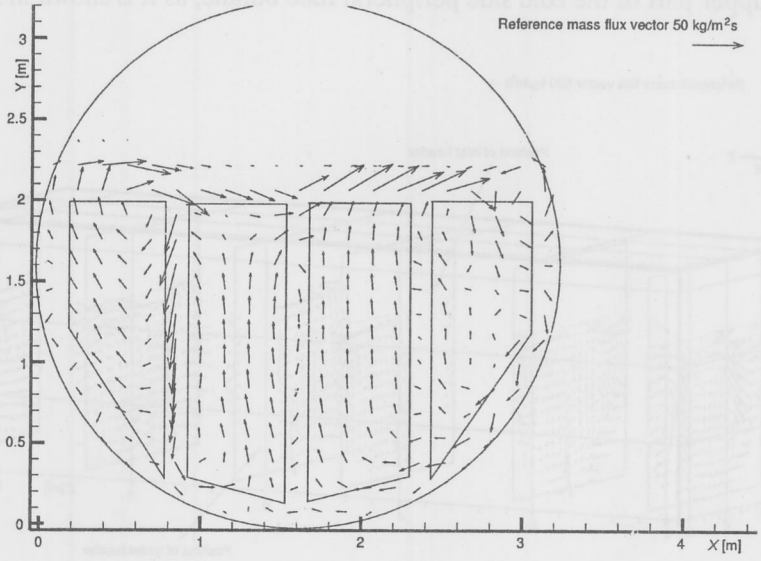

Figure 8. Water mass flux vectors in *X–Y* plane at $Z = 8.8$ m for WWER HSG

the position of z= 8.8 m the water downward flow is the highest at the passage between the central and peripheral tube bundles on the HSG hot side, Fig. 8, due to a lower difference of the hot and cold side heat fluxes in this plane near the HSG edge. The strong circulating flow of both phases is shown. At several locations steam phase is carried under by the strong water currents flowing from the swell level to the tube banks, as it is shown in the X–Y planes at z = 0.35, 2.4, 5, 6.6, 8.8 and 10.1 m in Fig. 9.

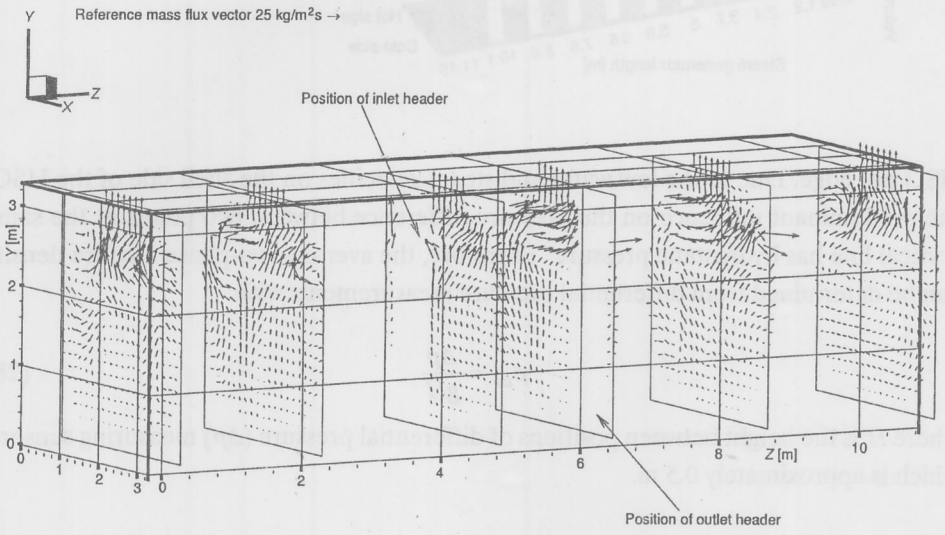

Figure 9. 3D view at steam mass flux vectors in several X–Y planes for WWER 440 HSG

The 3D-ANA code is capable of the swell level tracking. As it is shown in Figs. 6, 7 and 8 the water velocity at the swell level changes the flow direction from the upward to the downward direction. Above the swell level, the water velocity equals zero according to the simple physical condition that there is no liquid phase in that space. Thus, water and steam separation is modelled in the control volumes which comprises swell level. Accuracy of the swell level prediction is determined by the control volume height, which is 0.153 m in the presented computation.

Volumetric heating rates on the hot and cold sides along the HSG are shown in Fig. 10. A high imbalance of heat transfer from the primary to the secondary side of the HSG is shown. The ratio of the highest heating rate near the reactor coolant inlet header and the lowest heating rate near the outlet header is up to 4.4.

Computer results obtained with the 3D-ANA code are compared to the available experimental measurements presented in Table 2. Measurements at the WWER 440 HSG are taken in the corridors between tube bundles and bundles and HSG shell, at 0.7 m from the top row of the tubes and at 2 m distance from the feeding header to the

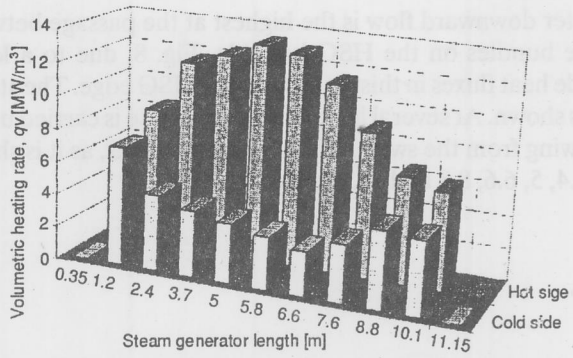

Figure 10. Heating rate per unit volume comprising tubes and two-phase mixture in WWER 440 HSG

HSG hot edge. Due to the low water and steam velocities on the shell side of the HSG, the predominant influence on the pressure difference between two points at the same vertical line has hydrostatic pressure. Therefore, the average two-phase mixture density can be determined from differential pressure measurements with

$$\rho_{av} = \frac{\Delta p}{gH} \tag{28}$$

where H is the height between positions of differential pressure (Δp) measuring sensors, which is approximately 0.5 m.

Table 2. A comparison of numerical and experimental data for WWER 440 HSG

Void	Experiment [16]	Experiment [3]	3D-ANA code
Cold side, corridor between peripheral bundle and shell – φ_1	0.25	0.27	0.26
Cold side, corridor between central and peripheral bundle – φ_2	0.42	0.38	0.29
Central corridor – φ_3	0.18	0.38	0.23
Hot side, corridor between central and peripheral bundle – φ_4	0.32	0.30	0.29
Hot side, corridor between peripheral bundle and shell – φ_5	0.32	0.25	0.28

Consequently, knowing the density, the average void can be calculated as follows

$$\varphi = \frac{\rho_{av} - \rho_1}{\rho_2 - \rho_1} \tag{29}$$

This method is widely used for the collapsed and swell level prediction [2, 13, 17, 18]. Experimental void fraction uncertainties are not reported in [3] and [16] for data in Table 2, but they might be estimated from other test facilities. In reference [17] is reported that pressurizer and steam generator collapsed levels were measured with an error of up to ±10%. Accepting the same error value in case of horizontal steam generator differential pressure measurements at the shell side absolute pressure of 4.6 MPa, the void uncertainty of approximately ±0.07 is derived. In [18] is reported that 40 kg/m^3 is adopted as a density uncertainty based on the differential pressure measurements on the secondary side of the vertical steam generator experimental model at the pressure of 6.4 MPa. This is equivalent to the void error of 0.07. Taking these values into account it might be assumed that the absolute error of the measured data in Table 2 is at least 0.07. The two sets of experimental data in Table 2 differ within the band of 0.07 for all locations except the central corridor location (φ_3), where the difference is 0.2. This high difference might be attributed to the fact that two measurements were performed at different times, within a few years, and that a number of circumstances might influence the measuring accuracy.

The absolute difference between measured data from [16] and calculated values is less than or equal to 0.05 for four points, while it is 0.13 only for the corridor between the central and peripheral bundle on the cold side (φ_2). The disagreement with the experimental data from [3] is also higher for the corridor between the central and peripheral bundles at the cold side (0.09), as well as for the central corridor (0.15). Existing discrepancies can be attributed to the complex water and steam 3D flow structure, which can have influence on both measured and computed data accuracy.

A comparison between 3D-ANA code void fraction results and experimental data for WWER 1000 HSG is given in [4 and 5]. The agreement is satisfactory. Besides, the WWER 1000 HSG numerical results have confirmed a number of mainly qualitative observations reported on swell level position, two-phase separation and fluid structure around the perforated plate in the WWER 1000 HSG. Results form [4 and 5], together with the data published in this paper, give a confidence that the 3D-ANA code results are a realistic representation of the complex two-phase flow structure on the HSG shell side.

So far as the authors of this paper are aware, experimental void fraction data are published for fifteen locations in the WWER 1000 HSG [13] and five locations in the WWER 440 HSG, [3 and 6]. Certainly, the complex three-dimensional two-phase flow field on the shell side of such a large component as the horizontal steam generator can not be viewed only on the basis of measuring points at several locations. Therefore, further experimental data from a real plant, scaled experimental facilities or separate effect tests are needed in order to provide experimental background for the HSG codes verification. Also, it is believed that joint efforts in experimental and analytical (numerical) investigations can lead to a better understanding of complex multidimensional thermal-hydraulic processes.

The 3D-ANA code algorithm for two-phase flow calculations has been first tested on the simple benchmark problems of a water expulsion by steam or steam expulsion by water in one-dimensional or two-dimensional geometry. But, the application of the 3D-ANA code to the HSG operating conditions has shown that one of the crucial

step is the modelling of interface momentum transfer, as it is presented in section 2.3.3. According to the present status in numerical heat and fluid flow abilities, this problem can be overcome mainly by the further experimental research.

Until now, 3D-ANA code calculations for both WWER 1000 and 440 were performed for nominal 100% load. A further verification of the 3D-ANA code application to the HSG thermal-hydraulic simulations will include partial loads. Experimental data for partial loads exist for both WWER 1000 and 440 steam generators.

Presented results have been obtained with the water mass inventory on the HSG shell side of 33 000 kg, as it is recommended in reference [19].

Conclusion

The numerical method and 3D Advanced Numerical Code (3D-ANA code) are presented for the simulation of three-dimensional two-phase flow on the secondary side of the horizontal steam generator. The modelling investigation has shown that the crucial phenomena for a proper prediction of void distribution, a two-phase velocity field and a swell level position is the interfacial momentum transfer. A combination of the Ishii-Zuber [9] and CATHARE code [12] interfacial friction correlation is proposed as appropriate for the HSG shell side thermal-hydraulic conditions. The results from this and previous papers [4, 5] show good agreement with the experimental data, especially regarding the complexity of multidimensional two-phase flow conditions, which has influence on both experimental and numerical results. Because of the limited data base for HSG thermal-hydraulics, there is a need for further code verification with a real plant or experimental test facility data, as well as with separate effect tests. The future work will include partial load simulations and a comparison with the available experimental data base for these conditions [13], as well as an application of the 3D-ANA code to kettle-reboilers and other industrial boilers with horizontal tube bundles.

Nomenclature

a [m^2/m^3]	– specific interfacial area
C_D	– drag coefficient
c_p [J/(kgK)]	– specific heat
D [m]	– diameter
d [m]	– tube inner Eq. (9) or outer Eq. (24) diameter
F [N/m^3]	– force of interaction
g [m/s^2]	– acceleration of gravity force
HSG	– horizontal steam generator
h [W/(m^{2}K)]	– heat transfer coefficient
h [kJ/kg]	– enthalpy
k [W/m^{2}K]	– heat transfer coefficient
M [kg/m^{3}s]	– volumetric mass source
m [kg/s]	– mass flow rate
Pr [ν/a]	– Prandtl number

p [N/m^2] – pressure
q [W/m^{3}s] – volumetric heat rate
Re [ud/ν] – Reynolds number
R_w [m^{2}K/W] – fouling resistance
S [m] – wetted inner surface per unit pipe length
T [°C] – temperature
t [s] – time
u [m/s] – velocity component in horizontal x direction, reactor coolant velocity inside tubes
V [m^2] – inner pipe volume per unit length,
v [m/s] – velocity component in vertical y direction
w [m/s] – velocity component in horizontal z direction
x, y, z [m] – Cartesian coordinates

Greek letters

α – volume fraction
Γ [kg/m^{3}s] – evaporation/condensation mass transfer rate
ζ – pressure loss coefficient
φ – steam volume fraction in space occupied by two-phase mixture, eq. (11)
ν [m^2/s] – kinematic viscosity
ξ – interfacial coefficient, eq.(18)
ρ [kg/m^3] – density
σ [N/m^2] – surface tension
τ [N/m^2] – shear stress

Subscripts

i – interface
p – particle
1 – water, primary side
2 – steam, secondary side
3 – tubes

References

[1] Wulff, W., Computational Methods for Multiphase Flow, *Proceedings*, the 2nd International Workshop on Two-Phase Flow Fundamentals, Rensselaer Polytechnic Institute, Troy, 1987
[2] Groburov, V. I., Zorin, V. M., Computer Modelling of Water Hydrodynamics of Steam Generator PGV-1000 (in Russian), *Teploenergetika* (1994), 5, pp. 22–29
[3] Melikhov, V. I., Melikhov, O. I., Nigmatulin, B. I., Thermal-Hydraulic Analysis of Horizontal Steam Generator, *Proceedings*, First International Symposium on Two-Phase Flow Modelling and Experimentation (Eds. G. P. Celata, R. K. Shah), Vol. 1, Edizioni ETS, Pisa, 1995, pp. 511–518
[4] Stevanović, V., Studović, M., Kiera, M., A 3D Numerical Simulation of Horizontal Steam Generator Thermal-Hydraulics, submitted for the 2nd International Symposium on Two-Phase Flow Modelling and Experimentation, to be held in Pisa , Italy, 1999
[5] Stevanović, V., Studović, M., Depisch, F., Kiera, M., 3D Modelling as a Support to Thermal-Hydraulic Safety Analyses with Standard Codes, Accepted for the 7th Int. Conf. on Nuclear Engineering, to be held in Tokyo, 1999
[6] Ishii, M., Two-Fluid Model for Two-Phase Flow, *Proceedings*, 2nd International Workshop on Two-Phase Flow Fundamentals, Rensselaer Polytechnic Institute, Troy, 1987

[7] Patankar, S. V., Numerical Heat Transfer and Fluid Flow, Hemisphere, 1980
[8] Rassohin, N. G., Nuclear Power Plants Steam Generators (in Russian), Atomizdat, Moscow, 1980, pp. 106
[9] Ishii, M., Zuber, N., Drag Coefficient and Relative Velocity in Bubbly, Droplet or Particulate Flows, *AIChE Journal*, *25* (1979), 5, pp. 843–855
[10] Medehekar, S., Amarasooriya, W. H., Theofanous, T. G., Integrated Analysis of Steam Explosions, *Proceedings*, 4th International Topical Meeting on Nuclear Reactor Thermal Hydraulics, Karlsruhe, Vol. 1, 1989, pp. 319–326
[11] Roser, R., Thonon, B., Icart, G., Mercier, P., Thermal Design of Kettle Reboilers: Experimental and Numerical Investigations, *Proceedings,* Third International Conference on Multiphase Flow (on CD ROM) (Ed. J. Bataille), Lyon, 1998
[12] Rousseau, J. C., Houdayer, G., Advanced Safety Code CATHARE Summary of Verification Studies on Separate Effects Experiments, *Proceedings*, 2nd International Topical Meeting on Nuclear Reactor Thermalhydraulics, Santa Barbara, 1983
[13] Ageev, A. G., Vasilyeva, R. V., *et. al.*, Investigation of Hydrodynamics of Steam Generator PGV-1000 (in Russian), *Elektricheskie stancii* (1987), 6, pp. 19–32
[14] Collier, J. G., Convective Boiling and Condensation, McGraw Hill, 1972, pp. 30
[15] David, F., THYC, a 3D Thermal-Hydraulic Code for Steam Generators, Heat-Exchangers and Condensers, *Proceedings*, 4th International Conference on Nuclear Engineering (Eds. A. S. Rao, R. B. Duffey, D. Elias), Vol. 1B (1996), pp. 509–516
[16] *** Experimental Data for WWER 440 Horizontal Steam Generator, Private Communication, Siemens AG, UB KWU, 1998
[17] Messie, A., Barre, F., Assessment of CATHARE LOFT Small Break Experiments, Seminaire CATHARE, Centre d'Etudes Nucleaires de Grenoble, 1985
[18] Sanders, B., Wittebrood, B., Eder, J., Ohlmer, E., Real Time Display of Mixture and Collapsed Levels within the LOBI-MOD2 Facility During Small Break LOCA Tests, *Proceedings,* Specialists Meeting on Small Break LOCA Analyses in LWRs, Vol. 1 (1985), Pisa, pp. 701–708
[19] Tuomisto, H., Secondary Side Water Inventory in the Loviisa Steam Generators, *Proceedings*, International Seminar on Horizontal Steam Generators Modelling (Eds. H., Tuomisto, H., Kalli, T., Kervinen), Vol. 1, Lappeenranta Univ. Technol. Res. Papers, Finland, 1991, pp. 31–36

Authors address:
Dr. V. D. Stevanović, associate professor
Prof. Dr. M. Ž. Studović, full professor
Faculty of Mechanical Engineering
80, 27. marta, 11000 Belgrade, Yugoslavia

Paper submited: November 25, 1998
Paper revised: January 15, 1999
Paper accepted: February 26, 1999